

# DIRECTIONAL SOLIDIFICATION OF FLAKE AND NODULAR CAST IRON DURING KC-135 LOW-G MANEUVERS

by

P. A. Curreri  
Space Science Laboratory  
Marshall Space Flight Center, Alabama 35812

and

D. M. Stefanescu and J. C. Hendrix  
University of Alabama  
University, Alabama 35486

## ABSTRACT

Alloys solidified in a low-gravity environment can, due to the elimination of sedimentation and convection, form unique and often desirable microstructures. One method of studying the effects of low-gravity (low-g) on alloy solidification has been the use of the NASA KC-135 aircraft flying repetitive low-g maneuvers. Each maneuver gives from 20 to 30 seconds of low-g which is between about 0.1 and 0.001 gravity.

A directional solidification furnace was used to study the behavior of off eutectic composition cast irons in a low-g environment. The solidification interface of hypereutectic flake and spheroidal graphite cast irons has been slowly advanced through a rod sample, 5 mm in diameter. Controlled solidification has been continued through a number of aircraft parabolas. The known solidification rate of the sample was then correlated with accelerometer data to determine the gravity level during solidification for any location of the sample. The thermal gradient and solidification rate were controlled independently. Three types of samples were run: hypereutectic flake graphite cast iron with low and high ( $\approx 0.2\%$ ) phosphorous content and hypereutectic spheroidal graphite cast irons obtained through treatment with metallic cerium. Samples run on the KC-135 aircraft exhibited bands of coarser graphite or of larger nodules usually corresponding to the regions solidified under low-g. Samples containing high P (used in order to determine the eutectic cell) exhibited larger eutectic cells in the low-g zone, followed by a band of coarse graphite.

## INTRODUCTION

It has been postulated [1] that gravity levels during solidification could have a significant effect on growth, macrostructural heterogeneity, and the size and distribution of macrophases in cast iron. During the solidification of hypereutectic irons, density differentials between light graphite material floating in heavier liquid could be expected to cause gravity-driven segregation. Other density differentials in the melt could be caused by the segregation of lighter alloying components such as sulfur or of heavier alloying components such as rare-Earth elements.

Thus, although cast iron is one of the most complex alloys used by modern industry, low-g experiments with cast iron could offer an excellent opportunity to study the effects of convection and sedimentation on alloy solidification. The complexity of the alloy combined with the demand for its usage (cast iron foundries produced 3.1 million tons of casting monthly worldwide in 1982, and over 600,000 tons in the United States [2]) make advances in cast iron casting technology of great interest to industry.

In June 1981, NASA began a Technical Exchange Agreement (TEA) with John Deere Company [3] to collaborate in a series of low-g solidification experiments of commercial cast iron utilizing NASA's low-g aircraft [4,5]. Of particular interest during this study was finding the effects of low-g on graphite nucleation and growth. The first series of experiments involved gas quenching of cast iron melts during the 20-40 sec, low-g time afforded by a KC-135 or F-104 low-g parabola. These experiments were partially successful [6,7]; however, many were inconclusive because complete solidification of the iron sample in the 20-40 sec low-g period could not be attained without producing predominantly white iron [8]. This paper describes the result of a parallel study undertaken, partially in support of the Deere/NASA TEA, in which directional solidification was employed. Directional solidification has many advantages over the quenched ingot methods for alloy solidification experiments, especially for low-g solidification experiments in the KC-135. In directional solidification, the solidification interface can be slowly advanced through a rod of the sample. Controlled solidification can continue through a number of aircraft parabolas. The known solidification rate (R) of the sample can then be correlated with accelerometer data to determine the gravity level during solidification for any location on the sample. The thermal gradient (G) and solidification rate can be controlled independently; whereas, for the quench ingot method the complexity of the three dimensional cooling problem makes their control very difficult. Knowledge of G and R allows quantitative expression of the influence of foundry variables on casting microstructures. The effect of the G/R ratio is summarized in Figure 1. It can be seen that as the G/R ratio is lowered or as the undercooling is increased the solidification interface changes from planar to cellular and then to dendritic. Eventually, heterogeneous nucleation will occur ahead of the solid-liquid interface (independent nucleation or endogeneous solidification) resulting in irregular interface due to grain nucleation and growth in microvolumes away from the interface. This last type of solidification is characteristic for cast iron solidifying with austenite-graphite eutectic. The thermal conditions associated with the solidification sequence described in Figure 1 are given in Figure 2.

## PROCEDURE

The basic experimental unit used in this research was a G.E. prototype ADSS furnace [9], which was modified for use in the NASA KC-135 low-g aircraft (Figure 3) primarily by adding a portable quench block water circulation system [10]. A thermal profile of an empty crucible measured with the maximum furnace temperature of approximately 1500°C is given in Figure 4 [10].

Different thermal gradients can be obtained by varying the maximum temperature in the furnace cavity, and the correlation between the thermal gradient in an empty crucible and the maximum furnace temperature is shown in Figure 5 [10]. Samples were directionally solidified during a series of up to 10 KC-135 low-g maneuvers. Figure 6 shows the KC-135 executing a maneuver, and Figure 7 illustrates schematically the gravity level variation during the maneuvers.

The flight experiments were run at constant R, with the furnace being translated vertically upwards while the KC-135 aircraft was flown through low-g parabolas.

## RESULTS AND DISCUSSION

A detailed discussion of the result of this study will be presented elsewhere [11]; in this paper it is intended only to highlight the findings relating to the effects of gravity on cast iron microstructure. The irons investigated [11] were commercial composition, hypereutectic, and fell within one of the following three categories: cerium containing cast irons, low phosphorus flake graphite (FG) irons, and high phosphorus flake graphite irons.

### Low Phosphorus Flake Graphite Irons

The low magnification metallographic structures of two hypereutectic iron samples from the same heat, directionally solidified during KC-135 low-g maneuvers, are given in Figure 8.

The gradient in the furnace was  $G = 327^{\circ}\text{C}/\text{cm}$ , and the growth rates were 5.5 and 1.1 mm/min respectively. The gravity environment for each region of the two samples can be read on the scales under the microstructures.

For the first sample, solidified at a rate of 5.5 mm/min, it can be seen that a very distinctive coarse graphite zone can be associated with the first low-g zone. Immediately, after the low-g zone, there is a zone of fine graphite before the graphite coarsening that characteristically occurs at the end of the sample.

A coarse graphite zone was also associated with the fourth low-g zone on the second sample, solidified at a rate of 1.1 mm/min. Then again, a lot of coarse graphite forms toward the end of the sample.

Since, in hypereutectic cast irons the partition coefficient of carbon between the solid and the liquid phases is higher than 1.0 and since coarsening due to sulphur segregation would not be expected to be as marked as that in Figure 8, the only viable explanation for the graphite coarsening seems to be the occurrence of flotation.

Coarsening of the graphite in some of the low-g zones could be explained by the following two hypotheses.

The first hypothesis is based on the lack of flotation in the low-g zone. This may allow primary graphite to be incorporated in the solidification front.

A second hypothesis is similar in nature with the one used to explain dendrite coarsening as a result of convective flow in a high-g environment. Since graphite is the leading phase in the solidification process of the austenite-graphite eutectic, in a high-g field, convection may break up the tips of the leading graphite and move them farther away in the liquid, where they can serve as nuclei for primary graphite and/or eutectic grains. In either case, the net result will be larger graphite flakes.

## Cerium Containing Spheroidal Graphite Irons

A composite microstructure of spheroidal graphite iron directionally solidified during KC-135 maneuvers is given in Figure 9. The furnace temperature for this sample was 1350° resulting in a gradient of 232°C/cm. The solidification rate between the melt interface and the first low-g zone was 6.33 cm/min (run up part), and 0.194 cm/min for the rest of the sample. It is obvious from Figure 9 that a high concentration of rather large nodules occurs in the region corresponding to the second low-g parabola, just before the third and fourth low-g parabolas, and at the fifth low-g parabola. A clearly defined flotation zone is obvious at the end of the sample, before the shut down of the furnace.

Also, a ground base experiment was run on a sample from the same heat under the same experimental conditions, except variable gravity. The structure along the sample was very similar to the one which can be seen on the run up part of the sample on Figure 9, with a rather uniform distribution of larger nodules between the small nodules.

The best explanation for the banding in the flight sample in Figure 9 seems to be flotation. The solidification process along the flight sample in Figure 9 was modeled using Stokes' law using the values given in Table I. It was found that the nodule size of the graphite bands was such that their flotation speed was slightly greater than the solidification interface speed in high-g but negligible compared to it in low-g. Thus, flotation and low-g zones can explain the occurrence of bands with big graphite nodules (flotation zone), both in the low-g zones and out of the low-g zones. It then seems reasonable to conclude from these results that graphite flotation in SG irons of high carbon equivalent composition can be prevented by solidifying the iron in a low-g environment.

## High Phosphorus Flake Graphite Cast Iron

High phosphorus iron was studied in order to study the influence of gravity on the grain size of cast irons. It is well known that irons containing high P contents will tend to solidify with rather high amounts of phosphide eutectic (steadite). Steadite tends to solidify at the grain boundaries and a special etching method allows for determining the eutectic grain size and shape. Low magnification composite micrographs of three high phosphorus samples from the same heat are given in Figure 10. The top and middle samples were solidified on the KC-135, the bottom was run as a one-g control.

The furnace temperature for all samples was 1500° resulting in a gradient of 284°C/cm. The solidification rate for all three samples (after a run up at 14.2 mm/min for the top sample) was 4.9 mm/min. For the control sample after the primary melt interface the structure changed gradually from type A graphite, no cells, to type D graphite, cells, and then remained unchanged for most of the sample, until the sample was pulled out of the furnace, resulting in a carbidic structure due to the high cooling rate.

In the second flight sample (middle Figure 10) the structure changed suddenly from type A graphite, no cells, to type D graphite, cells, at the first transition from the high-g to the low-g zone. Then, as the g environment was changed again the structure exhibited again type A graphite corresponding to the beginning of the high-g zone. A similar transition can be observed on first flight sample (top, Figure 10) in the middle of the first high-g zone after a low-g zone. Also, it is obvious that the cells are considerably larger in the first low-g zone than in the other regions of the sample.

A detailed evaluation on the eutectic cell count on the flight samples showed that despite a large scatter in the data the pattern for the variation of the eutectic cell count given in Figure 11 for the low-g and high-g zone seems to be implied. Thus, the data indicates that gravity enhances cell multiplication, and that the lack of convection in a low-g environment results in a lower number of eutectic cells during solidification.

This phenomena can be explained by a higher undercooling before solidification in the low-g zone. The experimental evidence for this is the abrupt transition from type A to type D graphite observed on both flight samples at the transition from some high-g zones to low-g zones (see Figures 10 top and middle, and Figure 12). Actually the transition is really from a planar solidification (no grain boundaries were revealed by deep etching) to an irregular solidification (Figures 1 and 2).

## CONCLUSIONS

In low-g environment, no flotation occurs even in SG irons with carbon equivalent as high as 5%. This opens the way for production of iron-carbon alloys with high carbon content (e.g. 10%), actually of iron-carbon composite materials in low-g environment. These materials could have a highly oriented structure as a result of directional solidification if flake graphite structures are solidified. Such a material will have a high thermal conductivity and strength in the direction of the heat flow, and low values for the above properties in a direction perpendicular to the heat flow. Also, composite Fe-C materials with uniformly dispersed spheroidal carbon particles could be produced by the same technique. By increasing the phosphorus content in hypereutectic FG irons, it was possible to document the influence of the low-g environment on the eutectic cells. It was observed that the eutectic cell count tends to decrease in a low-g zone, which means that convection currents existing in a high-g environment will produce cell multiplication by a mechanism not yet fully explained.

## REFERENCES

1. Frankhouser, W. L.: Materials Processing Threshold Report, II. Use of Low Gravity for Cast Iron Process Development. Final Report, Contract NAS8-33518, February 1980.
2. "17th Census of World Casting Production – 1982", Modern Casting, Vol. 73, No. 12 (December 1983), pp. 22-23.
3. Technical Exchange Agreement between National Aeronautics and Space Administration and Deere and Company in the area of Materials Processing in Low-Gravity, signed June 29, 1981.
4. Neu, L. R. J.: JSC Reduced Gravity Aircraft User's Guide. JSC-17385, May 1981.
5. Poorman, R. M.: F-104 Low-Gravity Calibration Test for Materials Processing in Space Precursory Experiments. NASA TM-78278, March 1980.
6. Stefanescu, D. M. and J. C. Hendrix: Report on KC-135 Cast Iron Samples No. Thur. No. 1 Through Fri. No. 5, Contract NAS8-34724, May 1982.
7. Fosbinder, L. L. and Klann, R. W.: NASA Solidification of Cast Iron in Zero Gravity. Deere and Co. Technical Report No. 173, August 1982.
8. P. A. Curreri, G. A. Smith, and G. Workman, "The Feasibility of Low-G Grey Solidification of Nodular Iron in the F-104 Experimental Furnace Package," NASA TM-82527, April 1983.
9. General Electric, Space Science Laboratory, Philadelphia, PA., NASA Contract Number NAS8-31536, (November, 1975).
10. P. A. Curreri, D. M. Stefanescu, and J. C. Hendrix, "Preliminary Science Report on the Directional Solidification of Hypereutectic Cast Iron During KC-135 Low-G Maneuvers, NASA TM-82528 (April, 1983).
11. Hendrix, J. C., P. A. Curreri, and D. M. Stefanescu, "Directional Solidification of Flake and Spheroidal Graphite Cast Iron in Low and Normal Gravity Environment," paper 84-99, 88th AFS Casting Congress, St. Louis, MO, May, 1984.

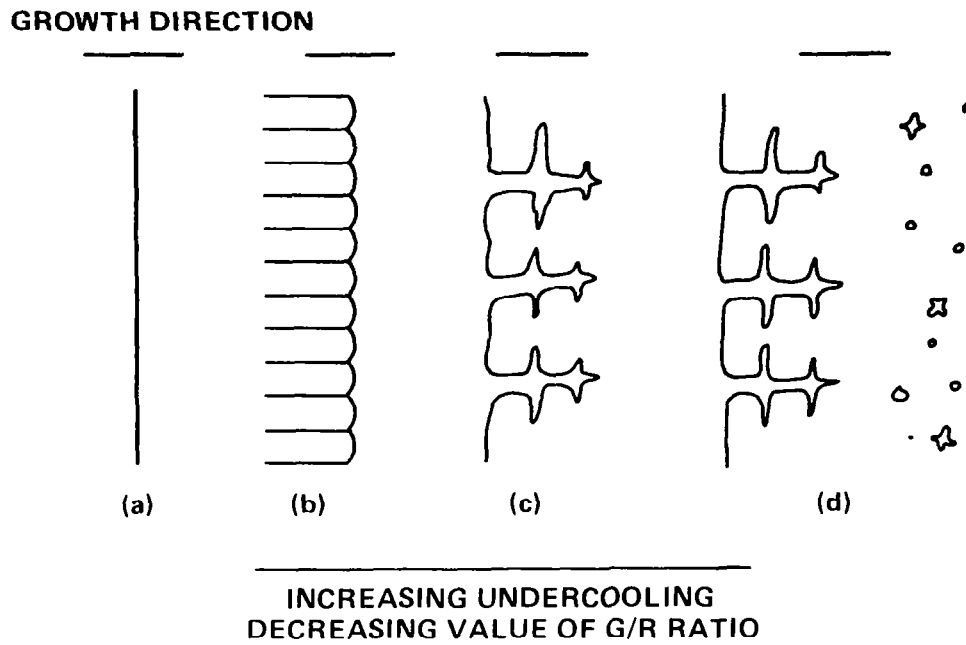


Figure 1. Influence of G/R ratio on interface morphology: (a) planar interface; (b) cellular interface; (c) dendritic interface; (d) irregular interface.

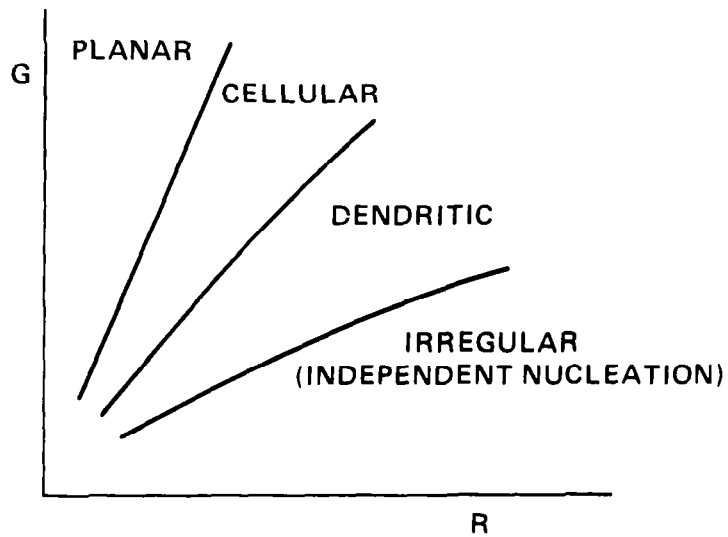


Figure 2. Influence of temperature gradient, G, and growth rate, R, on the interface morphology of a given alloy.

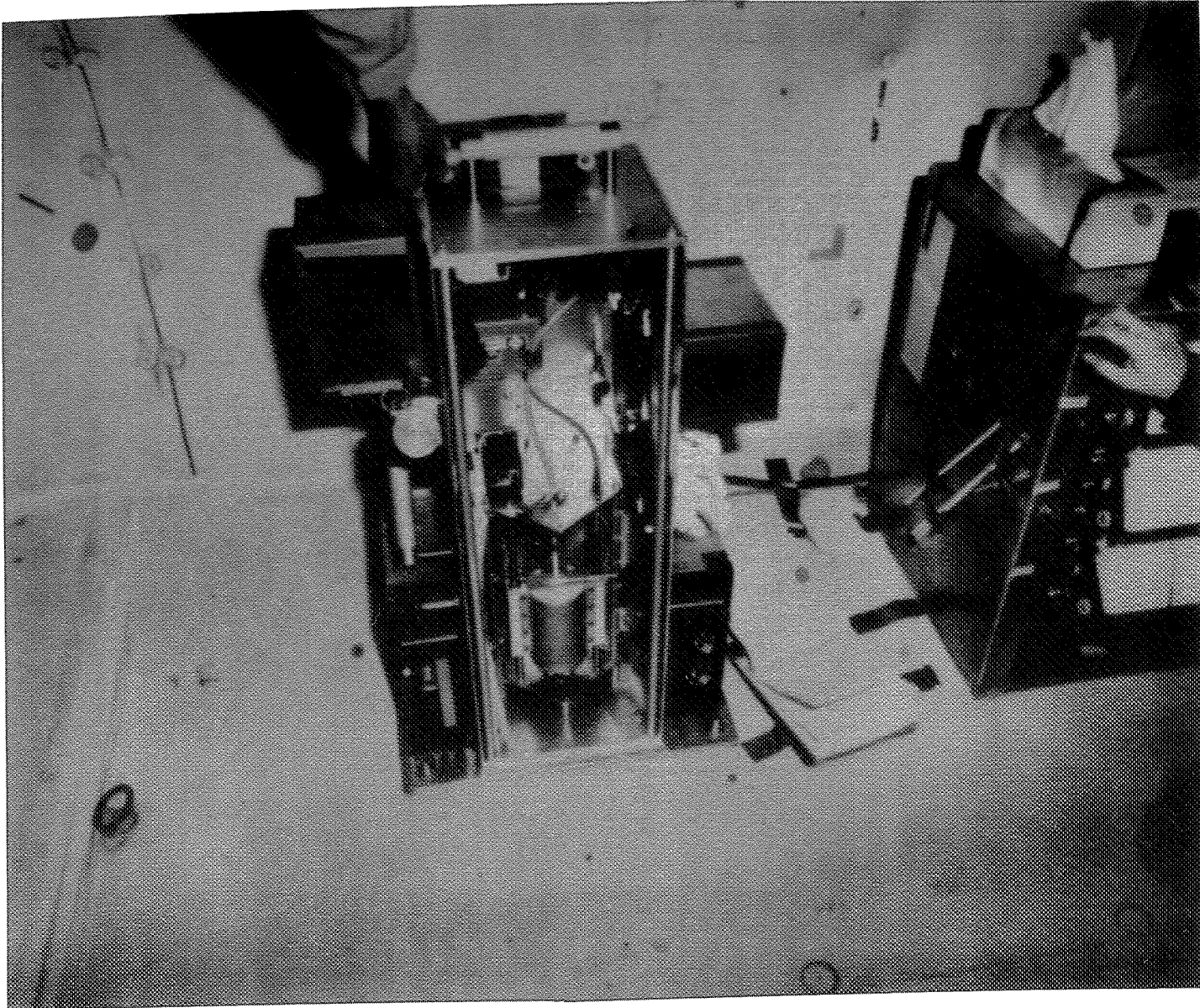


Figure 3. ADSS-P furnace installed in the KC-135 aircraft.



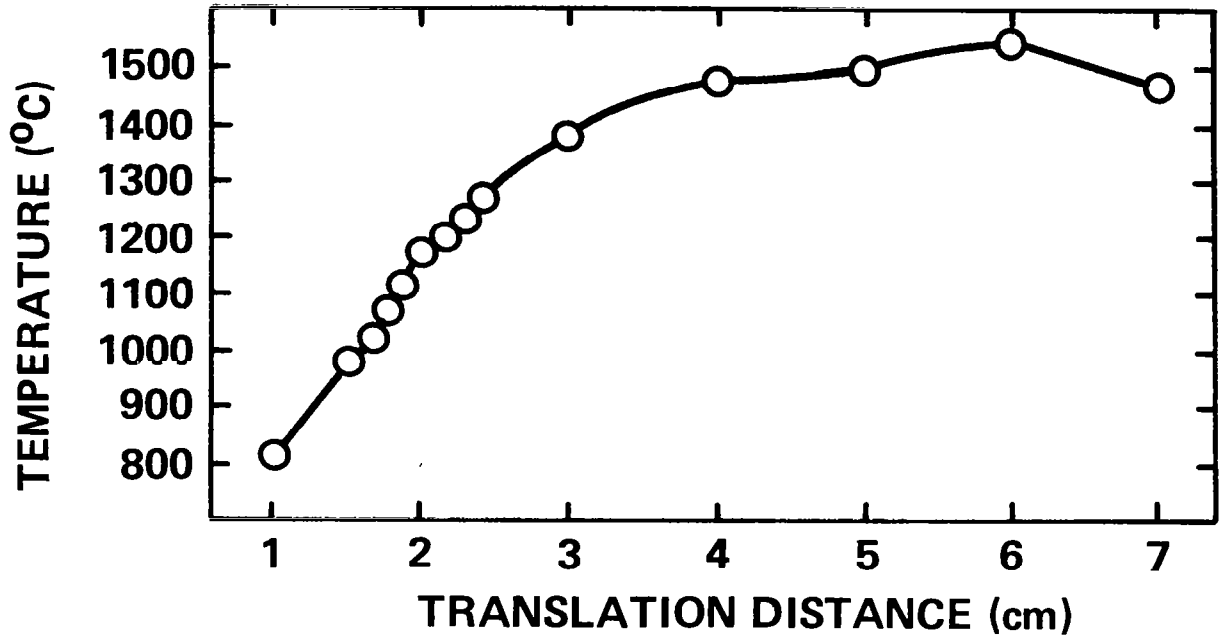


Figure 4. The thermal profile of an empty crucible for a furnace temperature of 1500°C.

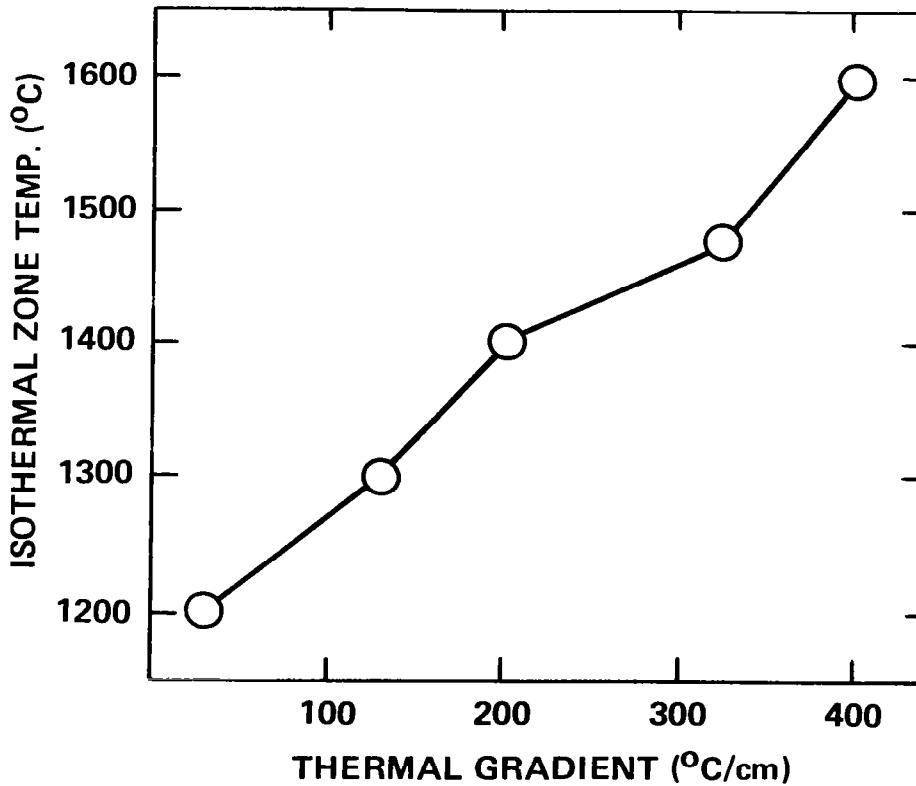


Figure 5. Thermal gradient (in an empty crucible) versus furnace temperature.

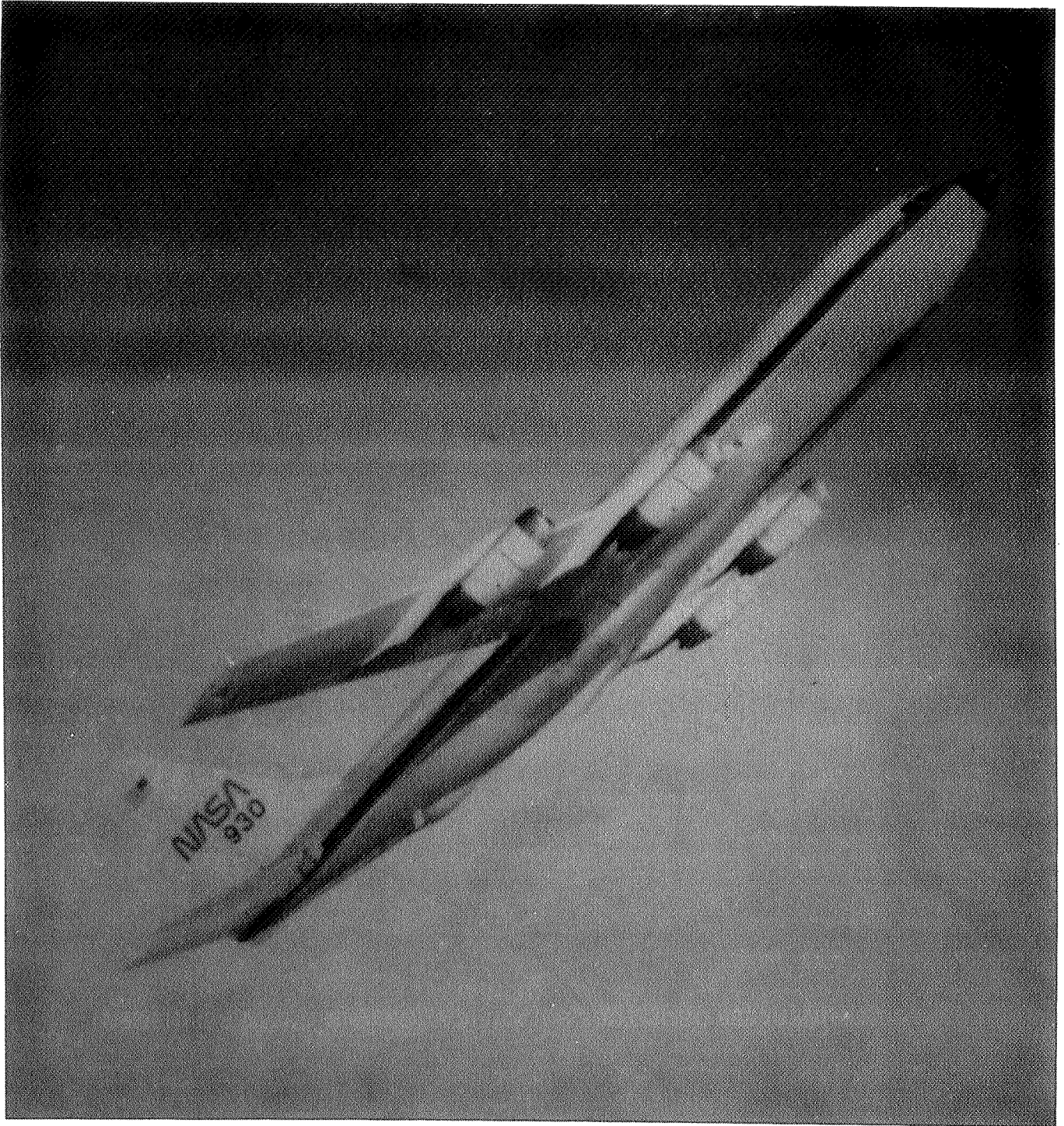


Figure 6. KC-135 aircraft during a low-g maneuver.

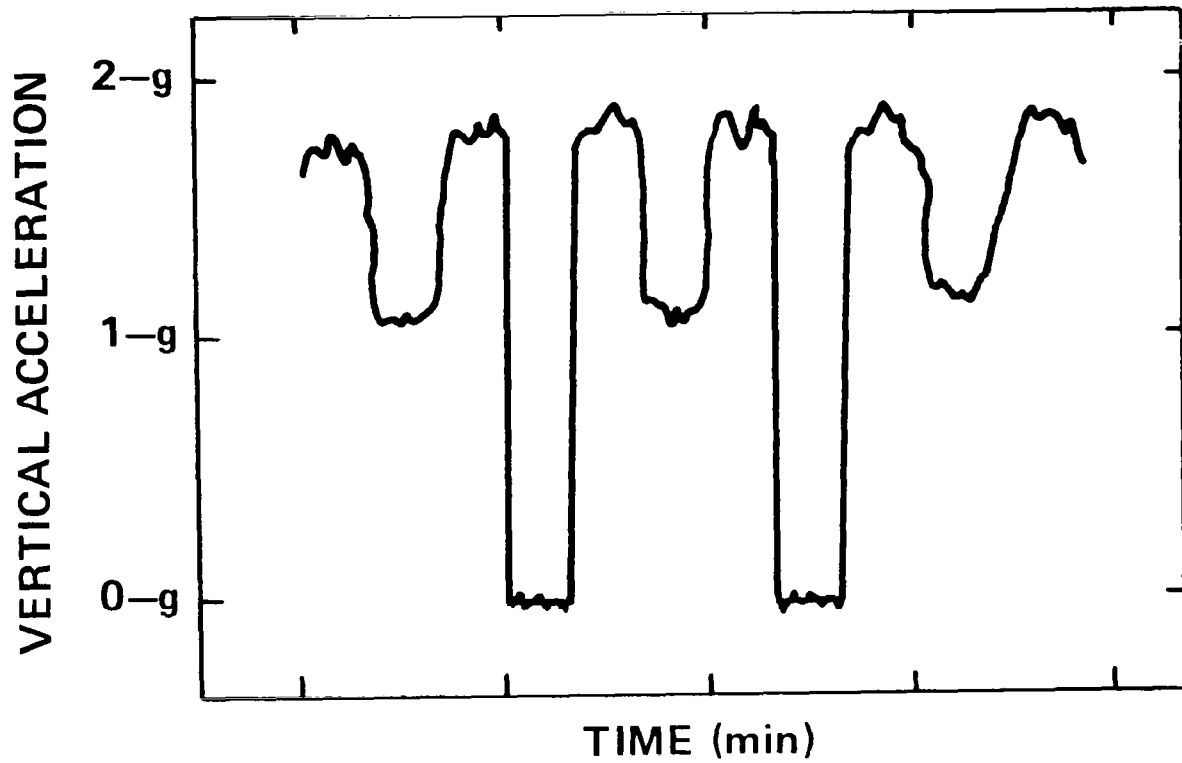
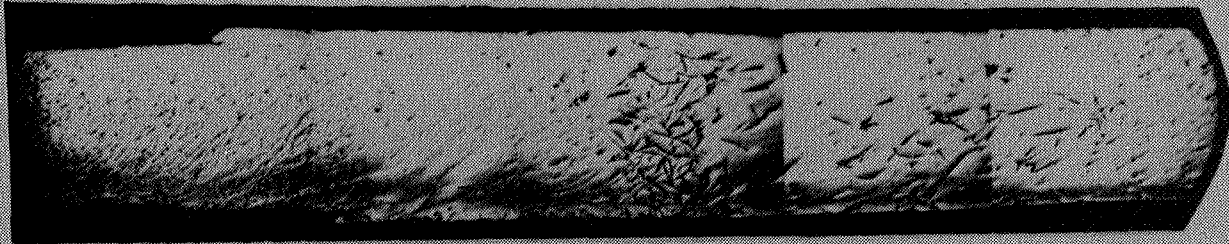


Figure 7. Schematic showing gravity level fluctuations during KC-135 multiple low-g maneuvers.

HYPEREUTECTIC CAST IRON  
SOLIDIFIED DURING KC-135 LOW-G MANEUVERS

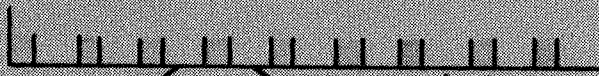
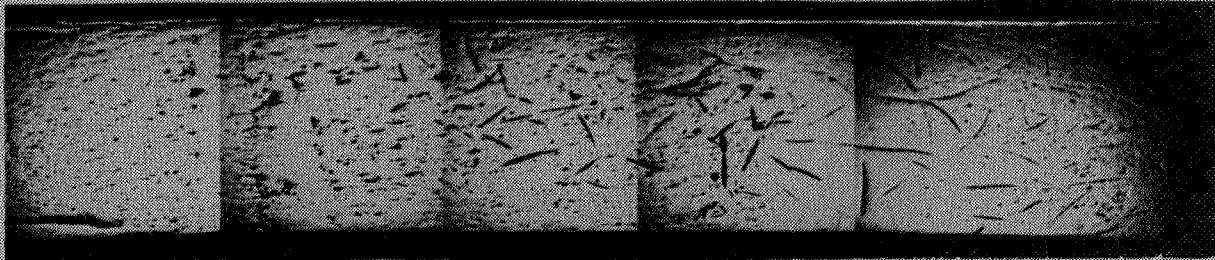
TRANSLATION RATE = 5.5 MM/MIN



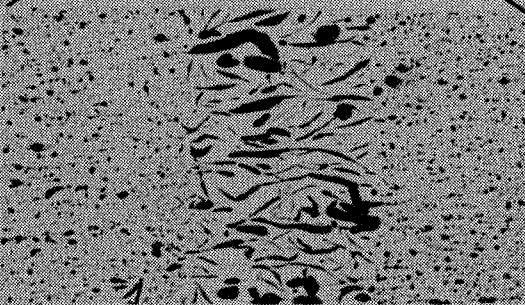
1 MM

LOW-G HIGH-G

TRANSLATION RATE = 1.1 MM/MIN



LOW-G  
HIGH-G



← INCREASED MAGNIFICATION  
5.5 x

Figure 8. Low magnification composite micrograph of the KC-135 directionally solidified hypereutectic iron flight samples.

**SOLIDIFIED DURING KC-135 LOW-G MANEUVERS**

**0.17% Ce Cast Iron**

**Translation Rate - 2.0 mm/min**

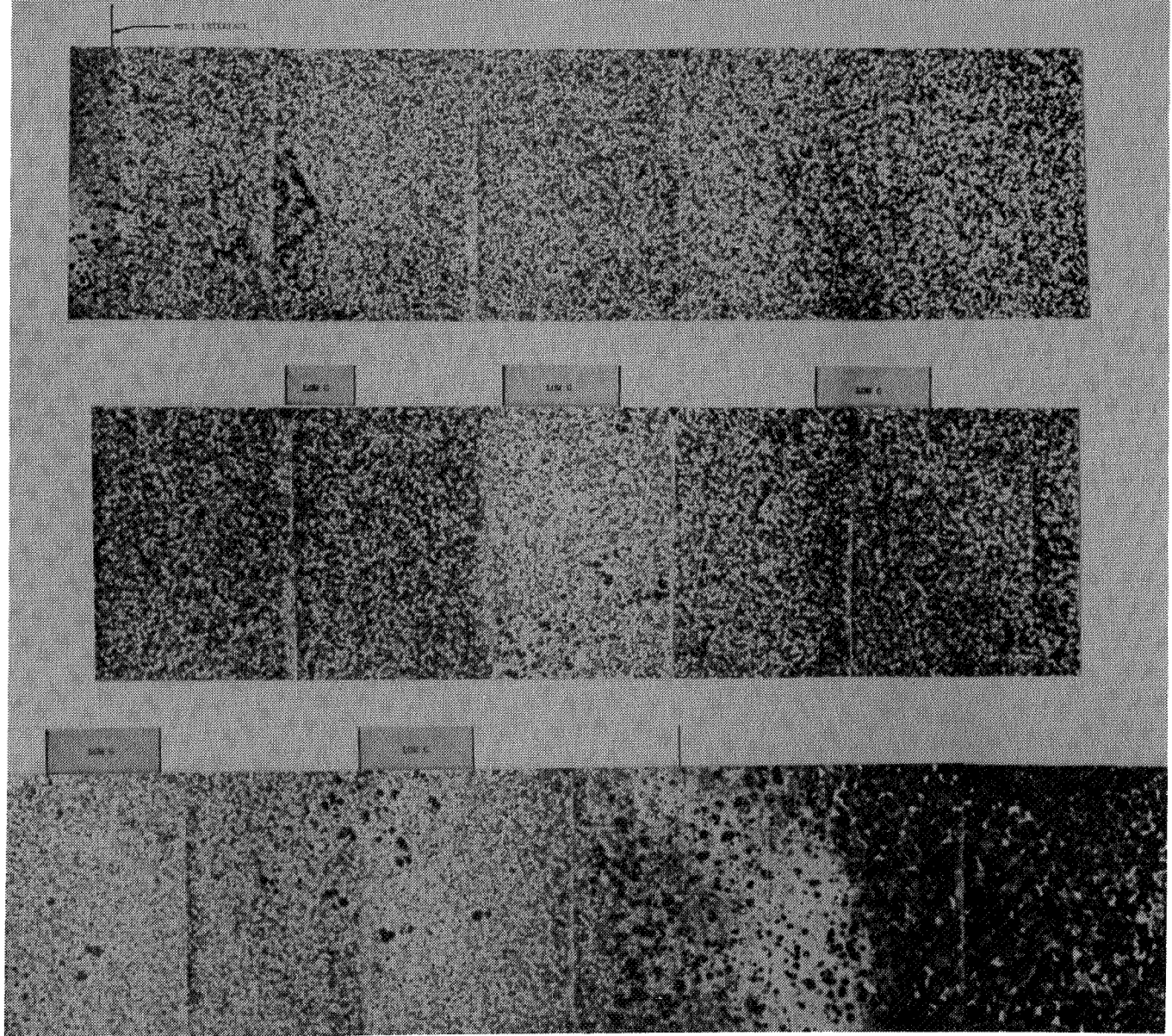


Figure 9. Low magnification composite micrograph of a KC-135 directionally solidified SG iron sample.

**SOLIDIFIED DURING KC-135 LOW-G MANEUVERS**

**0.21% P Cast Iron**

**Translation Rate : 4.9 mm/min**



Figure 10. Low magnification (originally x 12) composite micrographs of high phosphorus hypereutectic flake graphite iron samples: bottom – ground-based sample; middle – flight sample; top – flight sample.

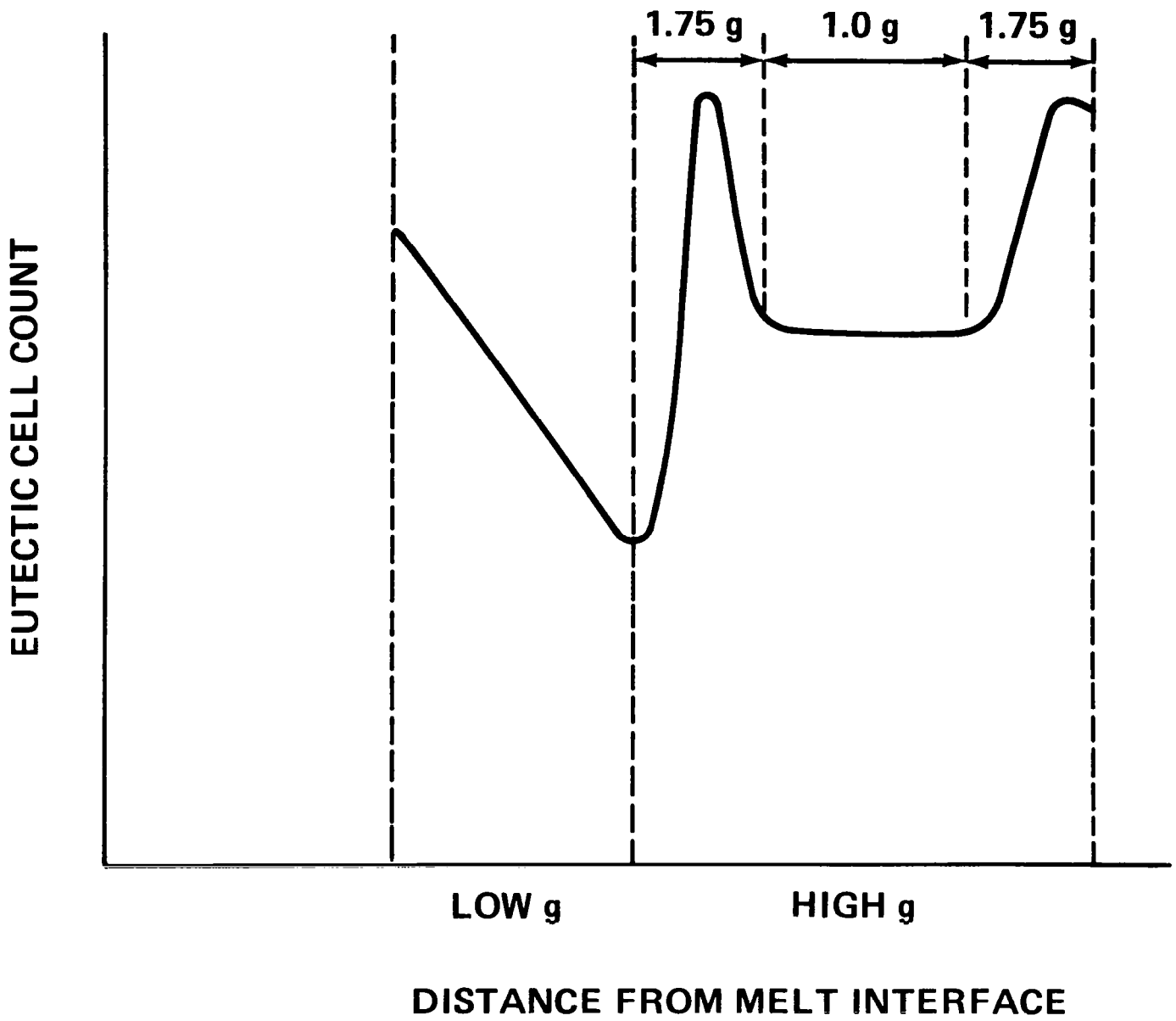


Figure 11. Schematic showing the influence of the gravity level on the eutectic cell count in high phosphorus flake graphite cast irons.

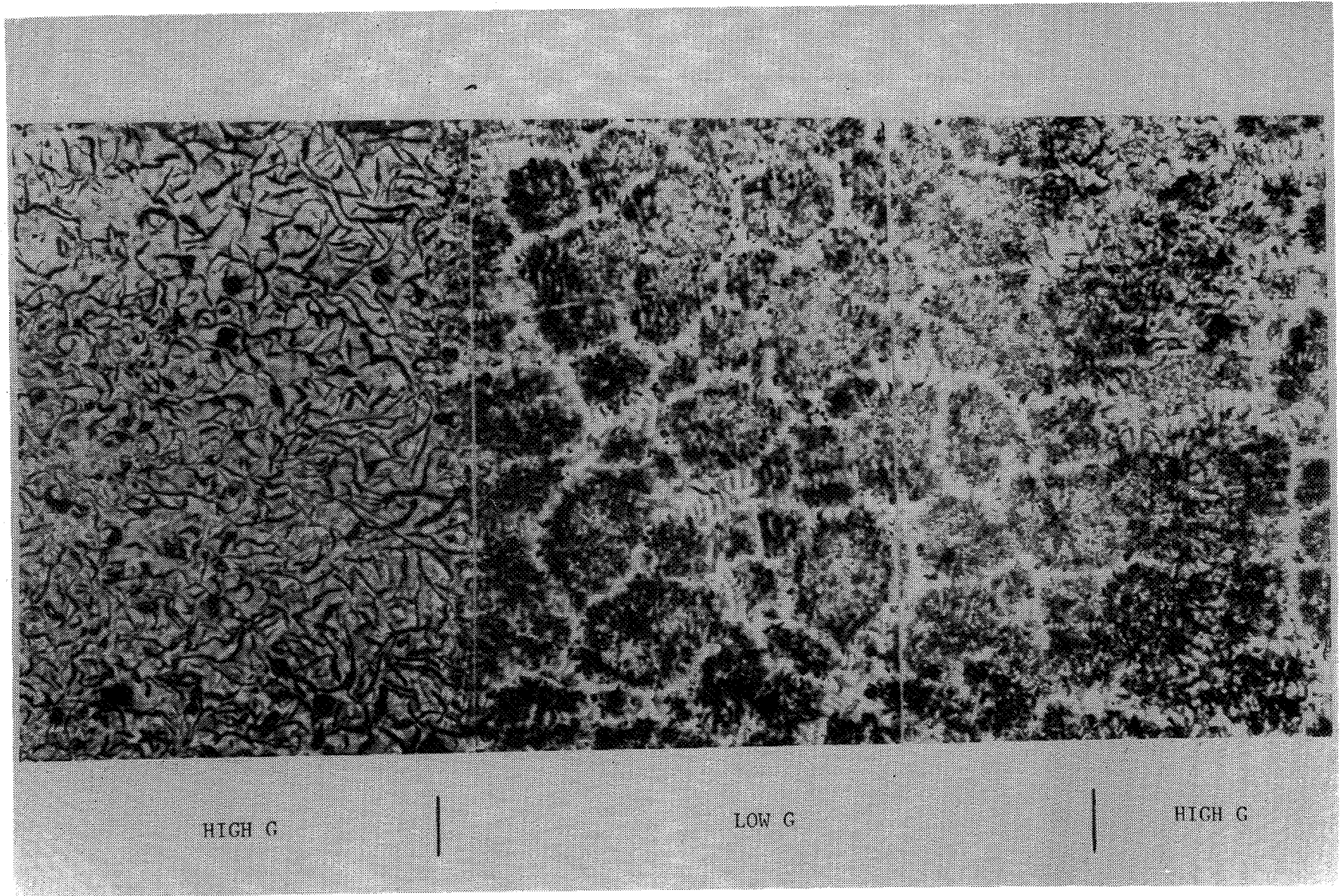
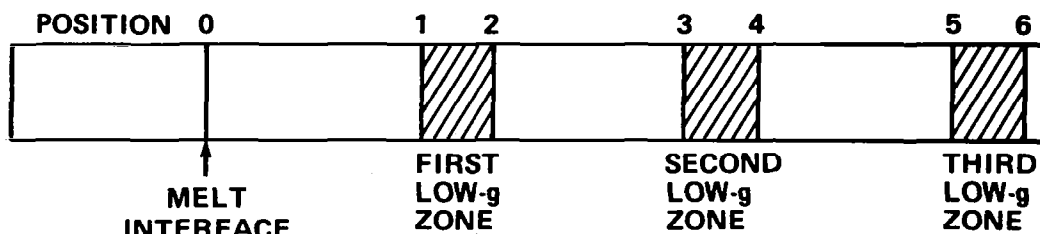


Figure 12. Transition from planar solidification (type A graphite) to irregular solidification (type D graphite) at a high-g to low-g transition on high phosphorus flight sample (Figure 10, top), Nital etched, x 50.



TABLE 1



STOKES' LAW GIVES: 
$$v = \frac{2}{9} r^2 (\gamma_2 - \gamma_1) \frac{g}{\eta}$$

- WHERE
- v : FLOTATION RATE, cm/sec
  - r : RADIUS OF SPHERICAL PARTICLE, cm
  - $\gamma_2$  : DENSITY OF THE LIQUID, g/cm<sup>3</sup>
  - $\gamma_1$  : DENSITY OF THE PARTICLE, g/cm<sup>3</sup>
  - g : ACCELERATION DUE TO GRAVITY, cm/sec<sup>2</sup>
  - $\eta$  : VISCOSITY OF THE LIQUID, CENTIPOISE

THE FOLLOWING VALUES WERE USED FOR CALCULATIONS:

- r = 0.00045 cm FOR THE RADIUS OF SG NODULES ON FIGURE 18
- $\gamma_2$  = 7 g/cm<sup>3</sup> FOR THE DENSITY OF CAST IRON
- $\gamma_1$  = 2.25 g/cm<sup>3</sup> FOR THE DENSITY OF GRAPHITE
- g = DIFFERENT VALUES CORRESPONDING TO DIFFERENT ZONES (SEE FOLLOWING TABLE)
- $\eta$  = 0.078 CENTIPOISE FROM REFERENCE (13)

TABLE WITH VALUES FOR THE GROWTH RATE R, ZONE LENGTH d, ACCELERATION DUE TO GRAVITY g AT VARIOUS POSITIONS ALONG THE SAMPLE:

POSITION	R, cm/sec	d, cm	g, cm/sec <sup>2</sup>
1	R <sub>01</sub> = 0.1055	d <sub>01</sub> = 0.95	g <sub>01</sub> = 1.49 x 981
2	R <sub>12</sub> = 0.0032	d <sub>12</sub> = 0.055	g <sub>12</sub> = 0
3	R <sub>23</sub> = 0.0032	d <sub>23</sub> = 0.12	g <sub>23</sub> = 1.32 x 981
4	R <sub>34</sub> = 0.0032	d <sub>34</sub> = 0.093	g <sub>34</sub> = 0
5	R <sub>45</sub> = 0.0032	d <sub>45</sub> = 0.161	g <sub>45</sub> = 1.24 x 981
6	R <sub>56</sub> = 0.0032	d <sub>56</sub> = 0.093	g <sub>56</sub> = 0